Received: January 4, 2022. Revised: March 24, 2022.

International Journal of
Intelligent Engineering & Systems

http://www.inass.org/

Implementation Optimal Location of STATCOM on the IEEE New England Power System Grid (100 kV)

Najib Ababssi[1]* **El alami Semma[1]** **Azeddine Loulijat[1]**

[1]*Laboratory of Engineering Industrial Management and Innovation, Faculty of Science and Technique, Hassan I University, Settat, Morocco*
* Corresponding author's Email: nababssi@gmail.com

Abstract: Voltage instability and voltage collapse are the serious problems that can occur due to reactive power deficits caused by increased load or contingencies. Detecting potential voltage collapse in power systems is essential to maintain voltage stability during high demand. The stability of power systems is an important issue in the planning and operation of these systems. This paper determined the optimal location and size of a FACT STATCOM device for improving the static voltage stability margin of a transmission system. The study network is the IEE New-England transmission network. The problem has been formulated as a multi-criteria optimisation with the objectives of maximising load margin, minimising power losses and minimising voltage deviation. The objective function of the problem is adjusted using the analysis and optimisation method (CPF). The appropriate values and placement for STATCOMs are found using the CPF method based on the objectives below. The proposed method is verified using a simulation test on the IEEE-100 kV network which is part of the IEEE- 39 bus New England power system. The simulation results showed the efficiency of the CPF for the nominal values and the optimal location of the STATCOM. The results showed that the improvement of the voltage stability margin, the voltage profile of IEEE-100 kV is increased and the power losses are reduced. Finally, STATCOM ensures the overall stability of the transport network.

Keywords: Flexible alternatif current transmission system (FACTS), Continuous power flow (CPF), STATic synchronous COMpensator (STATCOM), Power system analysis toolbox (PSAT) software, Theory of bifurcation, Stability.

1. Introduction

Today, the problems associated with the operation of electricity transmission and generation networks have assumed considerable importance. Faced with ever-increasing electricity consumption and very demanding environmental conditions, electricity networks are tending to grow and are becoming more and more meshed and interconnected. In addition, energy is transported over long distances using lines with high transmission capacity. This complexity of structure has many consequences. Such as : The difficulty of maintaining an acceptable voltage profile and keeping a stable network operating within contractual standards. The voltage stability of the network is then characterised by the ability of the network to maintain a voltage at the network buses within the specified operating limits. Voltage instability, on the other hand, is the result of the inability of the electrical network to supply the reactive power required by the load. Several widespread incidents around the world have been associated with voltage instabilities, resulting from poor reactive power management by the system [1]. There is a great need to improve the use and quality of electrical energy while maintaining its reliability, safety and stability [2-5]. Maintaining the voltage stability of the power system is one of the major problems due to frequent voltage collapse caused by disturbances, overloaded systems and operating conditions. Therefore, the voltage point is known as a high load point [6-8]. Similarly, the lack of capacity of the system to meet the reactive power demand is the main reason for the deterioration of the voltage profile [9]. Generally, the system is considered unstable when the voltage amplitude of any bus decreases and the reactive power increases for the same system bus [10-13]. However, the main way to avoid voltage dips is to decrease the reactive power load or increase the reactive power of systems [14-17].

To avoid the instability of electrical networks, it will probably be necessary to complement their action by implementing power electronic devices with high response speed, recently developed and known under the name FACTS (Flexible Alternative Current Transmission System), which translate a concept that groups together all the devices based on power electronics that make it possible to improve the operation of the electrical network. These FACTS devices provide a significant improvement in the voltage stability margin of large-scale power systems [18-22]. STATCOM, which is one of the FACTS devices, is mainly used to improve the voltage profile, where it is used to adjust the voltage by injecting a controllable voltage into the system [23].

In the existing literature, the optimal placement of FACTS devices is achieved using several analysis and optimisation techniques such as particle swarm optimisation (PSO), Newton-Raphson method and genetic algorithm (GA). In [9] the disadvantages of this method (PSO) are the high number of setting parameters and the use of archives. However, the use of archives introduces additional temporal and spatial complexities. This degrades the performance of these algorithms. In [20] the disadvantage of this method(NR) is its cost, it has to compute the Jacobian matrix at each iteration, and then factor it to solve the linear system. In [21] the disadvantages of this method(GA) is that it is computationally expensive, since it handles several solutions simultaneously. The adjustment of a GA is delicate. One of the most characteristic problems is that of genetic drift. Another problem arises when the right elements are no longer selected, and the algorithm no longer progresses.

In contrast to these three methods, continuous power flow (CPF) does not have the above-mentioned shortcomings. The CPF ensures greater accuracy in assessing the stability margin. The proposed method (CPF) finds the solutions of a series of successive power flows to determine the voltage profile as a function of the load evolution up to the collapse point. This advantage makes the CPF method more suitable for voltage stability analysis. Therefore, the continuous power flow (CPF) method was chosen.

In this paper, a methodology based on the (CPF) technique is proposed to find the nominal values and select the optimal location of the FACTS device. However, this paper focuses on the optimal selection and placement of the STATCOM compensator and its implementation in the IEEE- 39 Bus(100 kV) power system network to increase the stability margin, improve the voltage profile, reduce the active and reactive losses of the system and thus reduce power generation. Finally, all objectives are met and the total cost of the power system is reduced. STATCOM is able to improve the overall system performance.

The rest of the paper is structured as follows: the grid stability formulation, modelling of the FACTS device "STATCOM" coupled to the grid is explained in Section 2, the proposed method, load factor and power directions for voltage collapse study are presented in Section 3, simulation tests and discussion are provided in Section 4 followed by conclusions in Section 5.

2. Research method

In this section, the objective function of this document is to find the optimal location and ratings of the STATCOM device. This paper investigates the combination of three objective functions that maintain the bus voltage at the desired level, maximise the load margin, minimise the power flow in overloaded lines and minimise active and reactive power losses. As well as modelling a type of FACTS devices. In this paper, the overall performance of the power system is improved by using the shunt FACT device which is the STATCOM.

2.1 Load margin index (λ) and power flow

In this section, voltage stability indices are proposed with a standard power flow model. In this paper, bifurcation theory was used where the power flow equations of the system depend on a set of parameters with state variables, whose equation is given in Eq. (1) :

$$f(x, \lambda) = 0 \tag{1}$$

Where f is the power flow equation, x is the dependent variables and λ is the load factor, used to simulate the increase in load that leads to voltage collapse. In this paper the load factor has been calculated by the continuous power flow (CPF) technique. The parameter used to study the proximity of the system to voltage collapse is the load factor λ, which changes the powers of the generator and the load, thus the flow of the total powers in the transmission lines. The powers of the generator and the load can be expressed by the following Eq. (2),

[24]. In order to know the state of the electrical system for different load factors, the state variable must be added to Eq. (2).

$$\begin{cases} P_{G1} = (1+\lambda)(P_{G0} + P_S) \\ P_{L1} = (1+\lambda)(P_{L0} + P_D) \end{cases} \quad (2)$$

Where P_{G0} is the Active Power of the Generator, P_{L0} is the Active Power of the Load, P_S is the Supply bids and PD is the Demand bids.

The powers that multiply λ are called the steering powers. Eq. (2) differ from the model generally used in the analysis of continuous power flow (CPF). The total power gaps of the power flow problem are defined by the following Eq. (3), [24]. The system under consideration is summarised in Eq. (2):

$$\begin{cases} P_{G2} = (P_{G0} + \lambda P_S) \\ P_{L2} = (P_{L0} + \lambda P_D) \end{cases} \quad (3)$$

Where the load factor (λ) affects only the power variables P_S and P_D . The bifurcation point of the system is determined by systematically increasing the system load factor through the CPF. In typical bifurcation diagrams, voltages are plotted as a function of λ, thus obtaining the V(p) curves that determine the voltage collapse points. The indices 0, 1 and 2 denote the base case, the first point and the second point of power directions respectively. The proposed method for studying voltage collapse phenomena is based on the bifurcation theory using two approaches: the predictive step realised by the calculation of the tangent vector and the corrective step obtained either by a local parameterisation or by the perpendicular intersection as presented in Fig. 1. In the second approach, the FACTS device equations are added to the power flow equations. The new power flow equations are then used in the corrective step of the CPF process[25].

2.2 Power loss index (PLI)

The objective of reducing active and reactive power losses is achieved by choosing the best combination of variables, which minimises the total power losses of the power system. Based on this objective function, the active and reactive power losses are calculated with and without FACTS controller. The method proposed in this document is based on the CPF technique. Using the CPF, the active and reactive power losses are calculated. The behaviour of the test system considered with and without FACT, for different buses and different load conditions is studied. The PLI at the stability margin is minimised.

3. Continuous power flow calculation[5]

In this section, we focus on the continuous power flow method, using two approaches: the predictive step and the corrective step. The former is obtained by means of the tangent or tangent vector calculation, while the latter is obtained either through a local parameterization or at a perpendicular intersection. Fig. 1 illustrates the basic principle of continuous power flow calculation (CPF). The CPF method uses a prediction-correction scheme to solve the power flow equations. In general, the CPF consists of a prediction step performed by calculating the tangent vector and a correction step that can be obtained either by a local parameterisation or at a perpendicular intersection [26]. The method starts with a basic solution (λ= 0) and then estimates the next solution by prediction for a higher load factor. The estimated solution is then corrected by considering it as the initial solution of the program. The (CPF) method is widely recognised as a valuable tool for determining the V(P) curves of the power system [27]. Before applying the CPF method to study the voltage stability of the transmission network, it is essential to model the FACT device that is involved in this analysis. Fig. 2 shows the equivalent diagram of the STATCOM coupled to the grid to find the solutions of a series of successive power flows and determine the voltage profile as a function of the load evolution up to the collapse point.

3.1 Not predictor

The CPF method is based on the power flow Eq. (1). For λ= 0 (which corresponds to the base state), the prediction of the next solution is made by taking an appropriate step in the direction of the tangent vector to the next solution. The first step in the prediction process is to calculate the tangent vector. The tangent vector is obtained by deriving both members of Eq. (1). The CPF is then carried out in three stages, namely parametrisation, prediction and correction.

Parametrisation is mathematically a means of identifying each solution so that the solution so that the next or previous solution can be evaluated. The correction step obtains the new solution by correcting the predicted solution.

At the generic equilibrium point p, the following relation given in Eq. (4) applies to find this new solution by solving the system of said equation:

$$f(x_p, \lambda_p) = 0 \Rightarrow \left.\frac{df}{d\lambda}\right|_p = D_x f|_p \left.\frac{dx}{d\lambda}\right|_p + \left.\frac{df}{d\lambda}\right|_p = 0 \quad (4)$$

And the tangent vector can be approximated and given in Eq. (5):

$$\tau_p = \left.\frac{dx}{d\lambda}\right|_p \approx \frac{\Delta x_p}{\Delta \lambda_p} \quad (5)$$

From Eqs. (4) and (5), we have the equation given in (6):

$$\tau_p = -D_x f|_p^{-1} \left.\frac{\partial f}{\partial \lambda}\right|_p \quad (6)$$

With: $\Delta x_p = \tau_p \Delta \lambda_p$

With τ_p is the tangent vector, Δx_p is the deviation vector of the dependent variable at the generic point and $\Delta\lambda_p$ is the deviation vector of the load factor at the generic point.

At This point a control step size k should be chosen to determine the quantity Δx_p and $\Delta\lambda_p$, with a normalization to avoid large steps when $\|\tau_p\|$ is large, both equations are given in Eq. (7) and its representation is given in Fig. 1(a):

$$\begin{cases} \Delta\lambda_p = \frac{k}{\|\tau_p\|} \\ \Delta x_p = \frac{k\tau_p}{\|\tau_p\|} \end{cases} \quad (7)$$

Or decrease of λ. Fig. 2(a) shows a graphical representation of the predictor step.

3.2 Not corrector

Where $\|\cdot\|$ is the Euclidean norm and $k = \pm 1$. The sign of k determines the increase or decrease of λ. Fig. 1(a) shows a graphical representation of the predictor step.

For the corrective step, the set of n+1 equation are solved and are given in Eq. (8):

$$\begin{cases} f(x,\lambda) = 0 \\ \eta(x,\lambda) = 0 \end{cases} \quad (8)$$

After the prediction, the next step is the correction of the predate solution. For this a local parameterization is used in which the system of Eq. (1) is augmented by an equation which specifies the value of one of the state variables of the system. This state variable can be the amplitude of the voltage, the phase of the voltage or the load factor.

Where the solution of must be in the bifurcation manifold and is an additional equation to ensure a non-singular set at the bifurcation point. For the choice of there are two options: the perpendicular intersection and the local parameterization. In the case of the perpendicular intersection, whose representation is given by Fig. 1(b), the expression of η becomes Eq. (9):

$$\eta(x,\lambda) = \begin{bmatrix} \Delta x_p \\ \Delta \lambda_p \end{bmatrix}^T \begin{bmatrix} x_c - (x_p + \Delta x_p) \\ \lambda_c - (\lambda_p - \Delta\lambda_p) \end{bmatrix} = 0 \quad (9)$$

While for the local setting, either the parameter λ or the variable xi is forced to be a fixed value, so the equations as a function of λ and xi are given in Eqs. (10) and (11).

$$\eta(x,\lambda) = \lambda_c - \lambda_p - \Delta\lambda_p \quad (10)$$

$$\eta(x,\lambda) = x_{ci} - x_{pi} - \Delta x_{pi} \quad (11)$$

For the variable to be fixed, the choice must depend on the bifurcation manifold of f, as shown in Fig. 1(c).

The local parameterization is necessary to avoid the singularity of the Jacobian matrix at the point of maximum load, which causes numerical problems in the prediction and correction steps. In the correction step the value η is equal to the predicted solution.

3.3 Modelling of STATCOM

STATCOM is used for reactive power compensation, to suppress AC bus voltage fluctuations and to improve system transient voltage stability [28-31]. According to the IEEE, STATCOM is based on the injection of an alternating current into the controlled network through a coupling transformer [32-35]. The mathematical model in Fig. 2 represents the one-line scheme of an electrical network and a STATCOM installed in a transmission line. In general, the STATCOM voltage V_{sh} is injected in phase with the line voltage V_t and in this case there is no exchange of active energy with the network but only the reactive power that will be injected or absorbed by the STATCOM.

$$E_{sh} = V_{sh}(cos\delta_{sh} + j\, sin\delta_{sh}) \quad (12)$$

The current injected into the network by the STATCOM is given in Eq. (13):

$$I_{sh} = \frac{V_{sh} - V_t}{jX_t} \quad (13)$$

The transmission power between the two systems can be represented by the active power transmitted is given in Eq. (14):

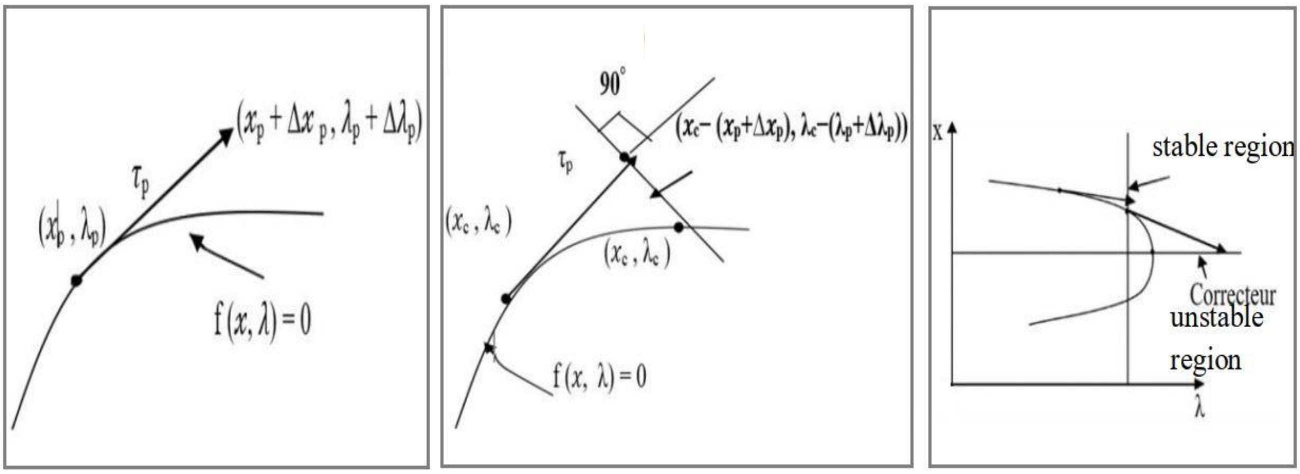

(a) (b) (c)

Figure. 1 Continuous calculation of the power flow for: (a) Not predictor obtained by means of the tangent parameterization, (b) Corrective step obtained by the means of perpendicular intersection, and (c) Corrective step obtained by using local parameterization

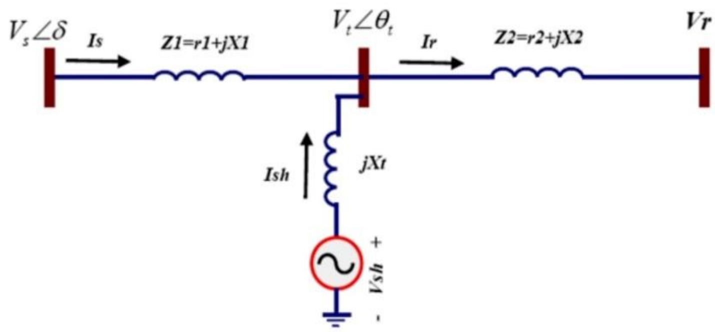

Figure. 2 Equivalent scheme of the STATCOM connected to the electrical network

$$P = \frac{V_t V_{sh}}{X} sin(\delta_t - \delta_{sh}) \quad (14)$$

The reactive power transmitted is given in (15):

$$Q = \frac{V_t^2}{X} - \frac{V_t V_{sh}}{X} cos(\delta_t \delta_{s_h}) \quad (15)$$

Where V_t,V_{sh} is the voltages at the bus,($\delta_t\delta_{sh}$) the angle between the voltage and X, line impedance. After some operations, the active and reactive power equations are given in Eqs. (16) and (17):

$$P_{sh} = V_t^2 g_{sh} - V_t V_{sh}(g_{sh} cos(\theta_t - \theta_{sh}) + b_{sh} cos(\theta_t - \theta_{sh})) \quad (16)$$

$$Q_{sh} = -V_t^2 b_{sh} - V_t V_{sh}(g_{sh} sin(\theta_t - \theta_{sh}) - b_{sh} sin(\theta_t - \theta_{sh})) \quad (17)$$

With: $g_{sh} + jb_{sh} = \frac{1}{Z_{sh}}$

Where, g_{sh} is the equivalent conductance of STATCOM, b_{sh} is the Equivalent susceptibility of STATCOM and Z_{sh} is the Equivalent impedance of STATCOM.

For an ideal STATCOM with no active losses, the reactive power in the power system is given in Eq. (18):

$$Q_{sh} = \frac{|V_t^2|}{X_{sh}} - \frac{|V_t||V_{sh}|}{X_{sh}} cos(\theta_t - \theta_{sh}) = \frac{|V_t^2|}{X_{sh}} - \frac{|V_t||V_{sh}|}{X_{sh}} \quad (18)$$

If $|V_t| > |V_{sh}|$, Q_{sh} becomes positive and STATCOM absorbs reactive power.

If $|V_{sh}| < |V_t|$, Q_{sh} becomes negative and STATCOM supplies reactive power.

Where, V_t is the Line voltage and V_{sh} is the STAT- COM voltage.

4. Results and discussion

The performance of the proposed method is evaluated using simulation tests on the IEEE 39 bus network which is part of a real US 100kV network and has 10 generators ($PGtotale$= 6.19 Gw,

Received: January 4, 2022. Revised: March 24, 2022.

$QGtotale$= 1.13 Gvar) and 39 buses including 19 load buses and 48 lines.The test system network is shown in Fig. 3. The software [PSAT][36] is used for the implementation of the CPF method. A case study is carried out, on 3 areas belonging to the same electricity network, to evaluate the proposed methodology before and after placement of the FACT device. Based on the proposed method, the values of the test network quantities are presented in Table 2.

4.1 Detection of the weakest bus

In order to study the voltage collapse point and to detect the weakest bus in the system, voltage stability margins are performed on the IEEE 39-bus test system (Fig. 3) with two types of stability indices: Load factor (λ) and active and reactive power losses. With respect to the first index, the system load is increased by the load factor (λ), starting from an initial stable operating point, until reaching the singularity point of the power flow linearization (λ_{max}). The incremental increase in system load while applying the first index leads to the response shown in Fig. 4(b), 4(c) and 4(d) of the 3 areas. From these figures, as well as Fig. 4(a) of the voltage profile, it can be deduced that the most fragile bus is the one that is closest to zero, (it is the one that tends to the voltage collapse point before the other buses (Fig. 5(b), which is the case for all three zones). As a result, it is the most sensitive bus to voltage variation in relation to reactive power. The maximum load point or bifurcation point when the Jacobian matrix is singular occurs at $\boldsymbol{\lambda}$=2.2806p.u. The overall rankings of the weakest buses in the system according to their response to voltage collapse without FACT are presented in Table 1.The reactive powers of the STATCOMs are obtained by the relations Eqs. (19) and (20):

$$Q_{max} = I_{L\,max} \times U_{max} \tag{19}$$

and

$$Q_{min} = I_{c\,max} \times U_{min} \tag{20}$$

from where:

$$X_{SL} = \frac{U_{max} - U_{min}}{I_{L\,max} - I_{c\,max}} \tag{21}$$

Where, I_{Lmax} is the Maximum inductive current, $I_{c\,max}$ is the Maximum capacitive current, Umax, Umin is the Voltage limits in regulation and X_{SL} is the Slope of the static characteristic in the control operating area.

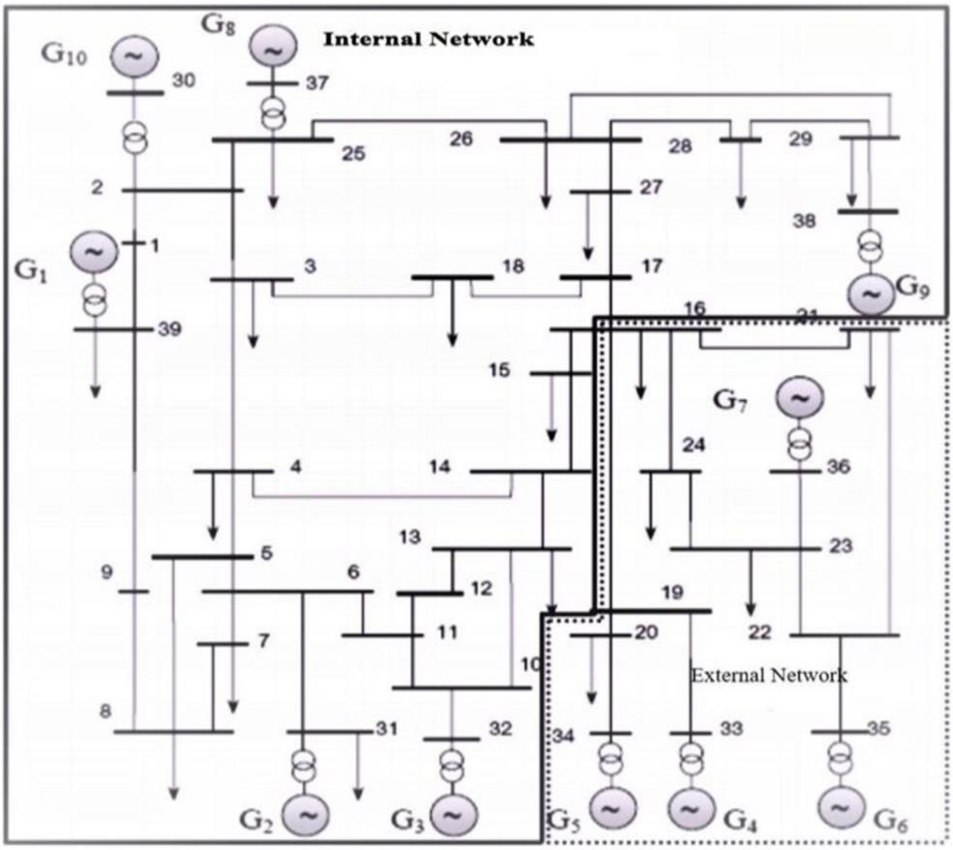

Figure. 3 The IEEE 39-Bus test network

 DOI: 10.22266/ijies2022.0630.37

Received: January 4, 2022. Revised: March 24, 2022.

Table 1. Weakest bus ranking in the 3areas

Area 1(Rank order)	**Area 2 (Rank order)**	**Area 3 (Rank order)**
8,7,5,6,4,12,14	3, 18, 17,27	15,16,24,21,28

The initial data used by the Continuation Power Flow (CPF) are values obtained from the Power Flow. The first execution of the power Flow has given results. The results of the parameters of the weakest bus of the 3 areas are in Table 2.

Table 2. Power flow results of the weakest buses in the 3 areas (Basic state)

Bus [p.u.]	**V phase[rad]**	**phase[p.u.]**	**P gen[p.u.]**	**Q gen[p.u.]**	**P load [p.u.]**	**Q load[p.u.]**
BUS03	0.77924	-0.68701	0	0	7.3428	0.05473
BUS04	0.65385	-0.74122	0	0	11.4019	4.1959
BUS5	0.66496	-0.62088	0	0	0	-0.44217
BUS6	0.67682	-0.55724	0	0	0	0
BUS7	0.63518	-0.7578	0	0	5.3315	1.9155
BUS08	0.63731	-0.80455	0	0	11.9035	4.0135
BUS12	0.63569	-0.43042	0	0	0.19383	2.0067
BUS14	0.67659	-0.57193	0	0	0	0
BUS15	0.69422	-0.62942	0	0	7.2972	3.489
BUS16	0.76104	-0.52743	0	0	7.5116	0.73656
BUS17	0.76356	-0.60644	0	0	0	0
BUS18	0.76264	-0.66831	0	0	3.603	0.68411
BUS21	0.77199	-0.35331	0	0	6.2482	2.6224
BUS24	0.7756	-0.51796	0	0	7.0372	-2.1025
BUS27	0.77377	-0.62843	0	0	6.4079	1.7217
BUS28	0.86833	-0.29065	0	0	4.6976	0.62939

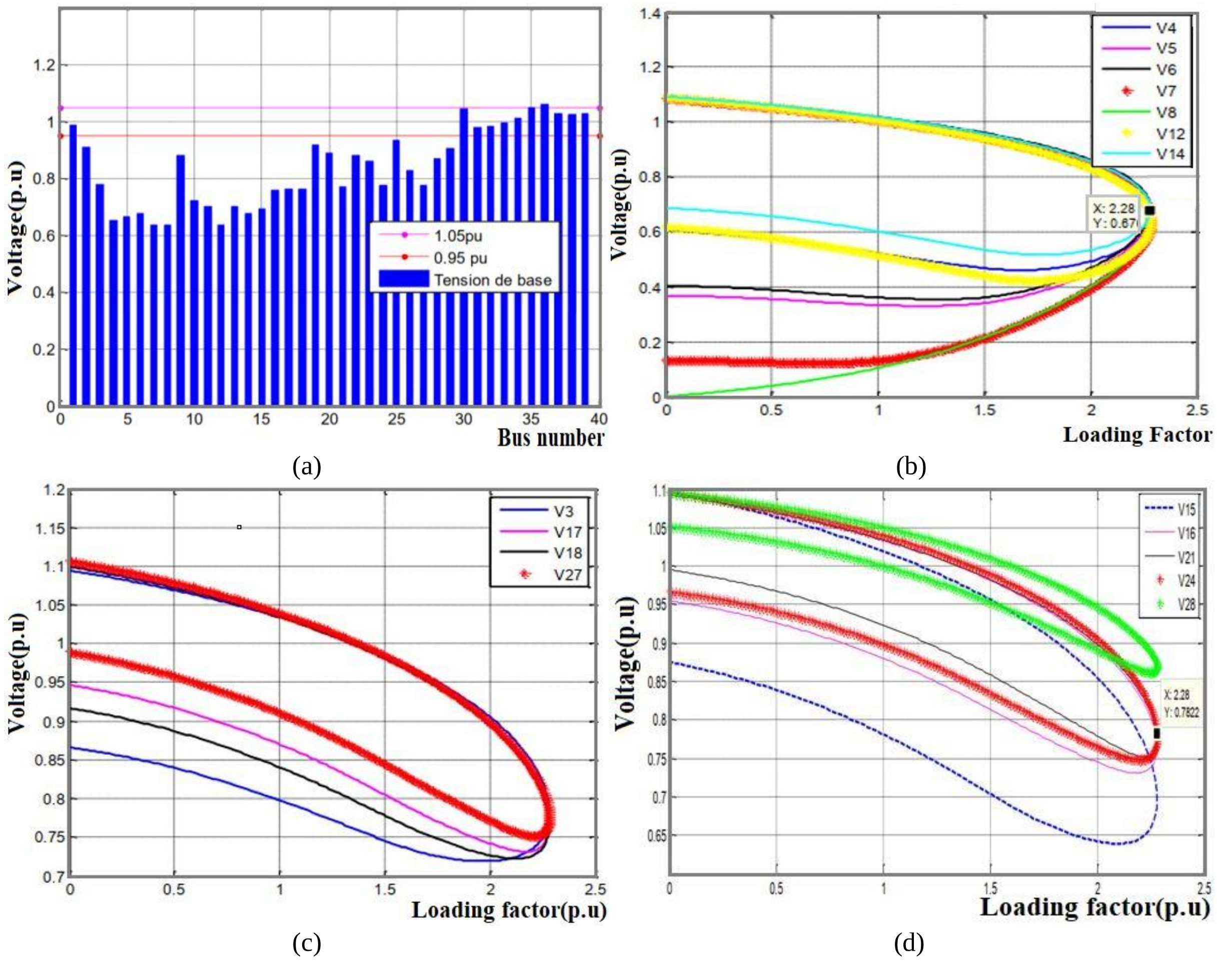

Figure. 4 (a) IEEE 39-bus network voltage profile and V(P) curves for (b) Area 1 of the system (basic state), (c) Area 2 of the system (basic state), and (d) Area 3 of the system (basic state)

Received: January 4, 2022. Revised: March 24, 2022.

4.2 Voltage profiles and power losses [37]

After determining the weakest bus of the test network. The method used based on the proposed CPF technique, to determine the optimal placement and nominal values of the FACT device is executed. At the first time, STATCOM is placed on bus 8 of area 1, it can be seen from Figure 5.a that the weakest buses in area1 have a better voltage profile than the baseline state and the load factor λ increases to the

Table 3. Total active and reactive power generation, total active and reactive power load and total active and reactive power losses before placing STATCOM

Total Generation		Total Load		Total Loses	
Active power[p.u.]	Reactive power[p.u.]	Active power[p.u.]	Reactive power[p.u.]	Active power[p.u.]	Reactive power[p.u.]
144.3043	121.2158	140.2543	31.686	4.05	89.5298

Table 4. CPF results of the weakest buses of the 3 areas (after placing STATCOM)

Bus [p.u.]	V phase[rad]	phase[p.u.]	P gen[p.u.]	Q gen[p.u.]	P load [p.u.]	Q load[p.u.]
BUS03	0.83248	-0.56145	0	0	7.4588	0.05559
BUS08	0.7846	-0.6495	0	1e-005	12.0915	0.93843
BUS15	0.75482	-0.5163	0	0	7.4124	3.5441

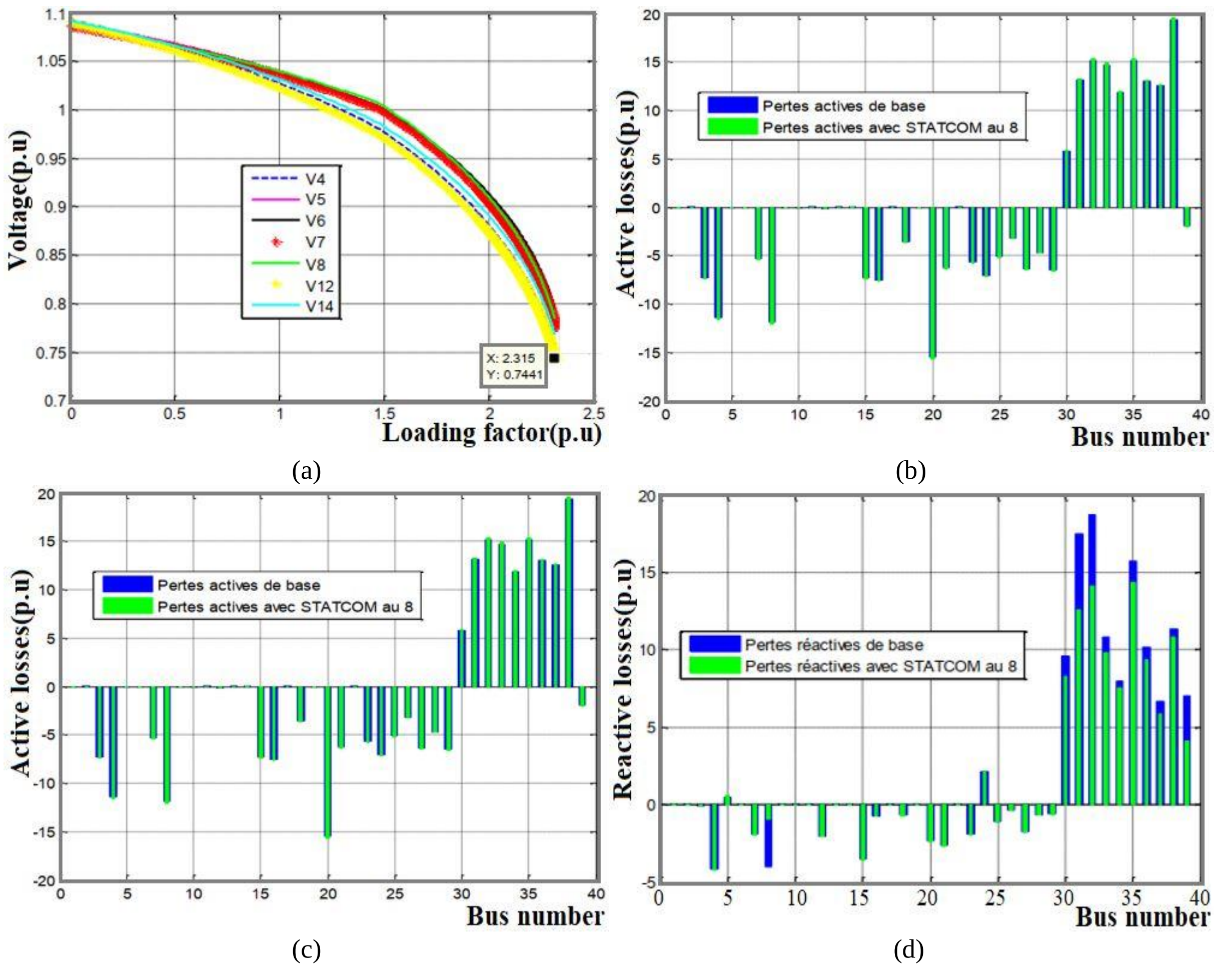

Figure. 5 (a) V (P) curve area 1 with STATCOM at bus 8, (b) System voltage profiles with STATCOM at bus 8 and powers losses profiles area 1With STATCOM at bus 8 for (c) Active loss, and (d) Reactive loss

Received: January 4, 2022. Revised: March 24, 2022.

maximum value. The bifurcation point occurs at a value $\boldsymbol{\lambda}$=2.31p.u. The value of the capacitive reactive power calculated from Eqs. (19) and (20) is -380MVAR /+ 420MVAR. The voltage profiles of the base case and the system with STATCOM are shown in Fig. 5(b). It is evident compared to the baseline state. This is due to the fact that STATCOM is installed at the weakest buses. On the other hand, the application of the active and reactive power loss index of the test system (with STATCOM placed at bus 8) while increasing the load, shows that the increase of losses in the vicinity of the collapse point is small, as shown in Fig. 5(c) and 5(d). Based on the proposed method, total active and reactive power generation, total load and total losses before STATCOM placement are presented in Table 3. from this figure that STATCOM provides a better voltage profile at the point of voltage collapse.

Based on the proposed method, the values of the test network quantities after STATCOM placement are presented in Table 4.

On the other hand, for the same STATCOM placed on bus 3 of area 2 and bus 15 of area 3, it is observed that this STATCOM offers the maximum of the load factor, as shown in Fig. 6.

In the second step, and since our goal through the search for the ideal location of the STATCOM device is to increase the voltage stability i.e. maximise the load factor λ of the system while controlling the voltage and minimising the active and reactive power losses, we place the same STATCOM on buses 3 and 15 belonging to areas 2 and 3 respectively, since these buses are the most fragile of these areas, and we observe the impact it can bring. The STATCOM placed on bus 3 of area 2 and bus 15 of area 3 offers the maximum load factor shown in Fig. 6. The V(p) curves with STATCOM on buses 3 and 15 are shown in Fig. 7(a) and 7(b), as well as their voltage profiles which are shown in Fig. 7(c) and 7(d). According to these figures, a slight voltage improvement on buses 2, 3 and 4 can be seen in the case of the STATCOM placed on bus 3. On the other hand, for the STATCOM placed on bus 15, the figures representing the voltage profiles show a slight drop in voltage on buses 5, 6, 7, 8, 9, 11 and 13 and an improvement for buses 15, 16, 17, 18 and 20. Table 3. Total active and reactive power generation, total active and reactive load and total active and reactive losses after placing STATCOM.

Table 5. Total active and reactive power generation, total active and reactive load and total active and reactive losses after placing STATCOM at bus 8 (Area 1).

Table 5. Total active and reactive power generation, total active and reactive power load and total active and reactive power losses after placing STATCOM

Total Generation		Total Load		Total Loses	
Active power[p.u.]	Reactive power[p.u.]	Active power[p.u.]	Reactive power[p.u.]	Active power[p.u.]	Reactive power[p.u.]
146.0172	102.682	142.4692	28.8773	3.5479	73.8047

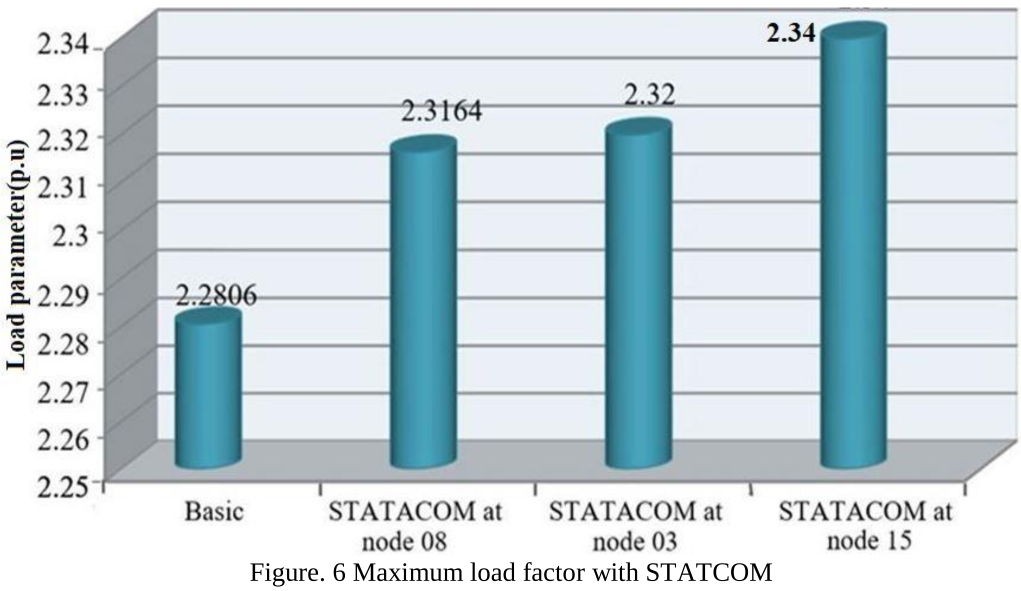

Figure. 6 Maximum load factor with STATCOM

 DOI: 10.22266/ijies2022.0630.37

Received: January 4, 2022. Revised: March 24, 2022.

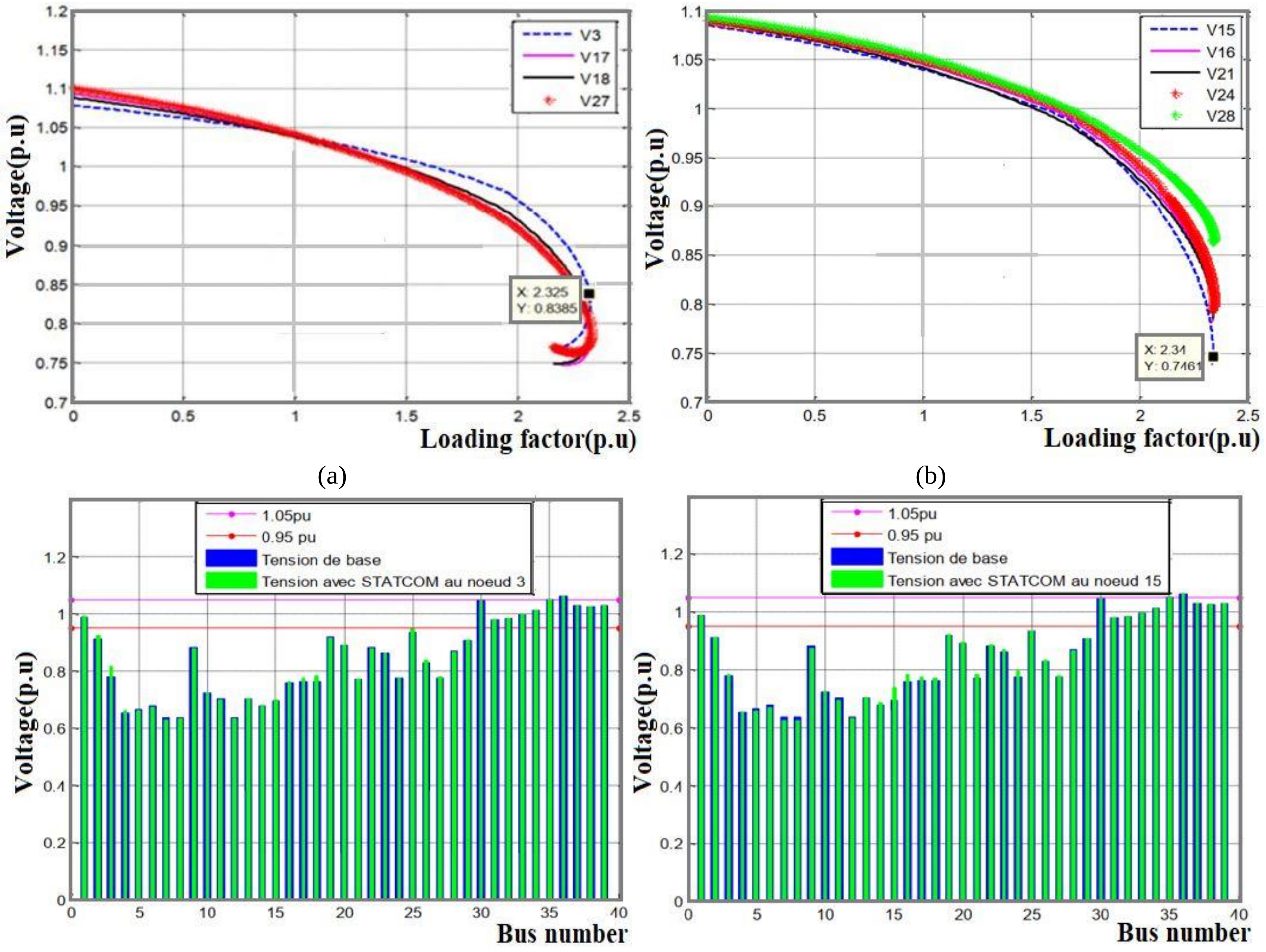

Figure. 7 V (P) curve with STATCOM for (a) area 2 at bus 3, (b) Area 3 at bus 15, System voltage profiles with STATCOM for (c) Bus 3, and (d) Bus 15

On the other hand, for STATCOM placed on buses 3 and 15 respectively, the increase in active and reactive power losses in the vicinity of the voltage collapse point is large, almost for all buses, as shown in Fig. 8(a) and 8(b), for STATCOM placed on bus 3, and Fig. 8(c) and 8(d), for STATCOM placed on bus 15. Fig. 9 shows the active and reactive power losses without and with the STATCOM device, so that the active power losses are reduced from 4.04(p.u) (basic state) to 3.54(p.u) (with STATCOM) while the reactive power losses are reduced from 89.53(p.u) (basic state) to 73.8(p.u) (with STATCOM), and this for the STATCOM placed on 8 bus. However, in the case of STATCOM placed on bus 3, the active power losses are increased from 4.04(p.u) to 4.18 (p.u) while the reactive power losses are increased from 89.53 to 92.62 (p.u).Whereas in the case of STATCOM placed on bus 15, it can be seen that the active power losses are increased from 4.04(p.u) to 4.15 (p.u) while the reactive power losses are increased from 89.53(p.u) to 92.49 (p.u). Fig. 10 shows the overall voltage ratio of the test system for the different STATCOM locations, where the bus 8 voltage is significantly improved from 0.61p.u to 0.7845 p.u.

Finally, proved that the application of the STATCOM device, placed on bus 8 of area 1 of the test network, by using the CPF technique yields very interesting results, improves the performance and efficiency of the IEEE 39 electric network (100 kV) compared with the references [9] and [21], achieves all the desired objective functions while controlling the real and reactive power flow in transmission lines trough the STATCOM device.

5. Conclusion

This paper proposes a methodology to detect, firstly, the weakest bus of electrical systems using two indices : the first is the stability margin(λ) or (Load Factor) and the second is the active and reactive power losses. The proposed method uses the Continuous Power Flow (CPF) technique to select the optimal location and ratings of the FACT device. The

Received: January 4, 2022. Revised: March 24, 2022.

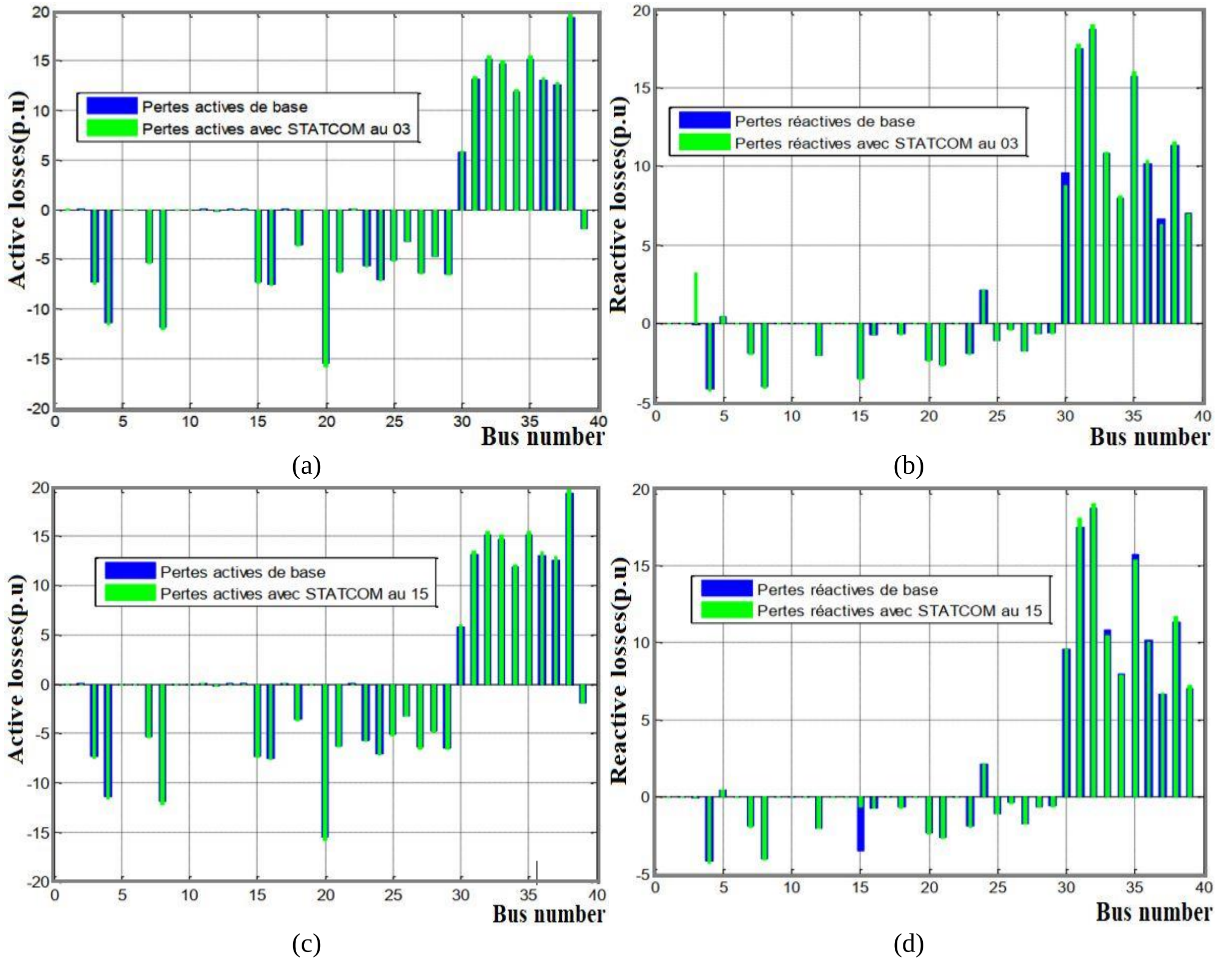

Figure. 8 Powers losses profiles in area 2 and 3with STATCOM for: (a) Active at bus 3 and (c) Active at bus 15, (b) Reactive at bus 3 and (d) Reactive at bus 15

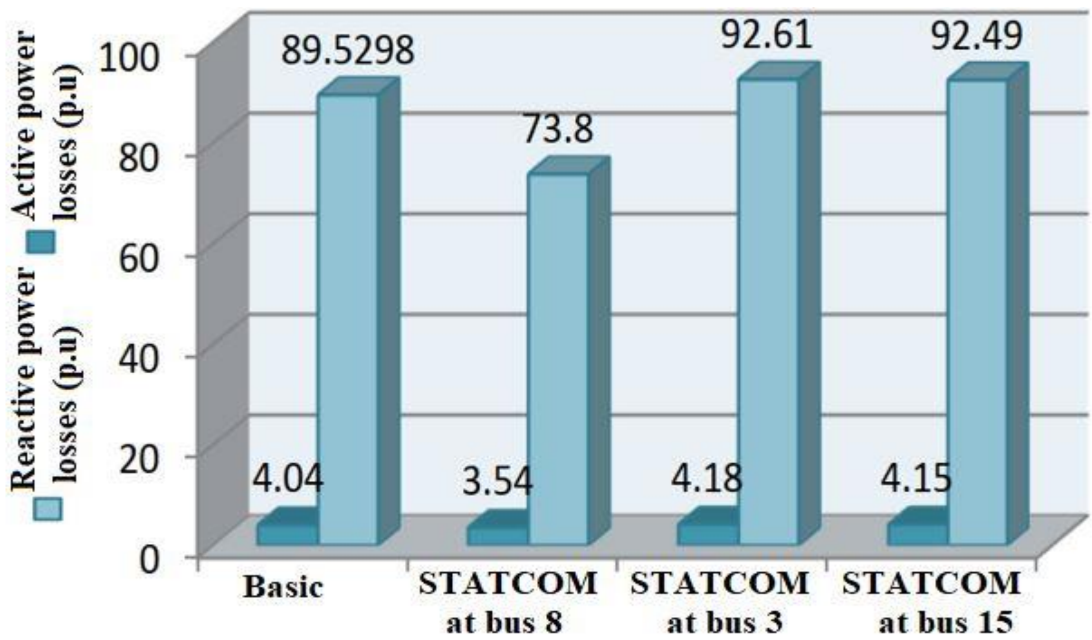

Figure. 9 Total active and reactive power losses for different STATCOM locations

Received: January 4, 2022. Revised: March 24, 2022.

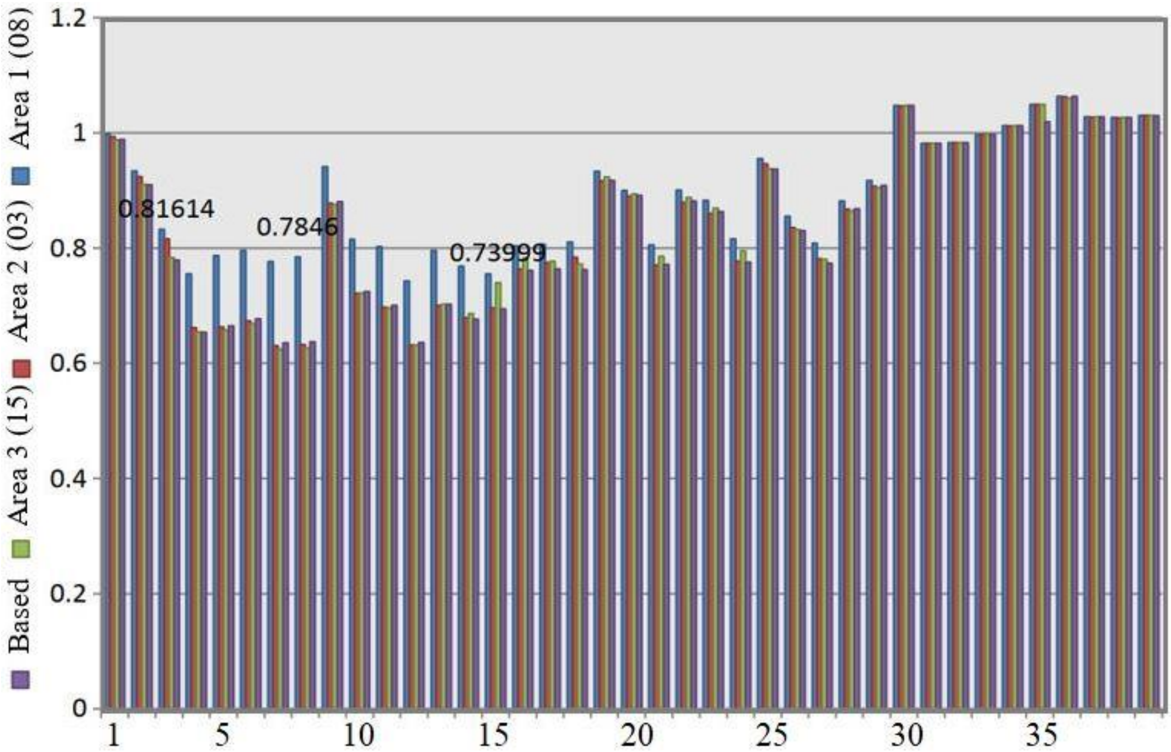

Figure. 10 Global voltage report for the different STATCOM locations

results show that the weakest bus in the 39-bus IEEE power network is bus 8. According to the proposed method, the optimal location for STATCOM is bus 8. STATCOM is capable of improving the voltage profile of the power system, reducing power losses and improving overall power system performance. On the other hand, the optimal location of STATCOM reduced the active and reactive power losses from 4.04(p.u) to 3.54(p.u) and from 89.53(p.u) to 73.8(p.u) respectively. The analysis and optimization results show that the CPF technique provides solutions when implemented for the FACT (STATCOM) device on bus 8. Thus, FACTS, in particular STATCOM, has a beneficial contribution in terms of network security.

This paper represents the first work that applies the analysis and optimisation method (CPF) together with the bifurcation theory that studies the phenomena of voltage collapse to find the optimal placement and ratings of the STATCOM device on the power system network (IEEE 39 bus 100 kV).

Conflicts of Interest

The authors declare no conflict of interest

Author Contributions

Najib Ababssi and El Alami Semma carried out a study on the impact of STATCOM on the voltage improvement of electrical networks and paper structure. Najib Ababssi has developed a mathematical model of the STATCOM device and implemented it in power flow software such as PSAT in order to study its impact on voltage collapse. Ababssi Najib and Azeddine Loulijat wrote the paper. Najib Ababssi and Azeddine Loulijat contributed to reviewing the paper. All authors read and approved the final manuscript.

References

[1] M. I. Ahmed, S. Saurabh, and R. Kumar, "GA Based Optimal STATCOM Placement for Improvement of Voltage Stability", In: *Proc. of 2020 Int. Conf. Renew. Energy Integr. into Smart Grids A Multidiscip. Approach to Technol. Model. Simulation, ICREISG 2020*, pp. 43-48, 2020.

[2] S. W. Mohod and M. V. Aware, "A STATCOM - Control scheme for grid connected wind energy system for power quality improvement", *IEEE Syst. J.*, Vol. 4, No. 3, pp. 346-352, 2010.

[3] M. Darabian, A. Jalilvand, A. Ashouri, and A. Bagheri, "Stability improvement of large-scale power systems in the presence of wind farms by employing HVDC and STATCOM based on a non-linear controller", *Int. J. Electr. Power Energy Syst.*, Vol. 120, No. November 2019, p. 106021, 2020.

[4] S. Opana, J. K. Charles, and A. Nabaala,

 DOI: 10.22266/ijies2022.0630.37

Received: January 4, 2022. Revised: March 24, 2022.

"STATCOM Application for Grid Dynamic Voltage Regulation: A Kenyan Case Study", In: *Proc. of 2020 IEEE PES/IAS PowerAfrica, Power Africa 2020*, 2020.

[5] Y. S. Maru, "Performance Study of A System with Optimal Location of STATCOM Device using MPMJ Algorithm under Normal Operating Conditions", *International Journal of Engineering Research & Technology*, Vol. 10, No. 01, pp. 682-691, 2021.

[6] S. Abe, Y. Fukunaga, A. Lsono, and B. Kondo, "Power System Voltage Stability", *IEEE Power Eng. Rev.*, Vol. PER-2, No. 10, pp. 39-40, 1982.

[7] P. Kundur, G. Andersson , J. Paserba, N. D. Hatziargyriou, "Definition and classification of power system stability", *IEEE Trans. Power Syst.*, Vol. 19, No. 3, pp. 1387-1401, 2004.

[8] S. Kihwele, "Enhancement of Voltage stability margin using FACTS devices for 132 kV Tanzania grid network", In: *Proc. of ICEIC 2019 - Int. Conf. Electron. Information, Commun.*, pp. 1-3, 2019.

[9] G. A. Salman, H. G. Abood, and M. S. Ibrahim, "Improvement the Voltage stability margin of Iraqi power system using the optimal values of FACTS devices", *Int. J. Electr. Comput. Eng.*, Vol. 11, No. 2, pp. 984-992, 2021.

[10] T. He, S. Kolluri, S. Mandal, F. Galvan, and P. Rastgoufard, "Identification of weak locations in bulk transmission systems using Voltage stability margin index", In: *Proc. of 2004 International Conference on Probabilistic Methods Applied to Power Systems*, pp. 878-882, 2004.

[11] S. A. Soliman, H. K. Temraz, and S. M. E. Khodary, "Power system Voltage stability margin identification using local measurements", In: *Proc. of LESCOPE 2003 - 2003 Large Eng. Syst. Conf. Power Eng. Energy Futur. Conf. Proc.*, pp. 100-104, 2003.

[12] S. Chansareewittaya and P. Jirapong, "Power transfer capability enhancement with multitype FACTS controllers using hybrid particle swarm optimization", *Electr. Eng.*, Vol. 97, No. 2, pp. 119-127, 2015.

[13] S. K. A. Hassan and F. M. Tuaimah, "Optimal location of unified power flow controller genetic algorithm based", *Int. J. Power Electron. Drive Syst.*, Vol. 11, No. 2, pp. 886-894, 2020.

[14] A. Wiszniewski, "New criteria of Voltage stability margin for the purpose of load shedding", *IEEE Trans. Power Deliv.*, Vol. 22, No. 3, pp. 1367-1371, 2007.

[15] A. R. Phadke, M. Fozdar, and K. R. Niazi, "A New Technique for on-line Monitoring of Voltage Stability Margin Using Local Signals", In: *Proc. of Fifteenth National Power Systems Conference (NPSC), IIT Bombay*, pp. 488-492, 2008.

[16] R. Mahanty and P. Gupta, "Voltage stability analysis in unbalanced power systems by optimal power flow", *IEE Proceedings - Generation, Transmission and Distribution*, Vol. 151, No. 3, pp. 201-212, 2004.

[17] M. Nizam, A. Mohamed, and A. Hussain, "Dynamic Voltage collapse prediction on a practical power system using power transfer stability index", In: *Proc. of 2007 5th Student Conf. Res. Dev. SCORED*, No. December, pp. 0-5, 2007.

[18] N. K. Sharma, A. Ghosh, and R. K. Varma, "A novel placement strategy for FACTS controllers", *IEEE Trans. Power Deliv.*, Vol. 18, No. 3, pp. 982-987, 2003.

[19] M. A. Kamarposhti, M. Alinezhad, H. Lesani, and N. Talebi, "Comparison of SVC, STATCOM, TCSC, and UPFC controllers for static Voltage stability evaluated by continuation power flow method", In: *Proc. of 2008 IEEE Electr. Power Energy Conf. - Energy Innov.*, 2008.

[20] G. A. Salman, M. H. Ali, and A. N. Abdullah, "Implementation Optimal Location and Sizing of UPFC on Iraqi Power System Grid (132 kV) Using Genetic Algorithm", *Int. J. Power Electron. Drive Syst.*, Vol. 9, No. 4, p. 1607, 2018.

[21] G. A. Salman, "Impleme- ntation SVC and TCSC to Improvement the Efficacy of Diyala Electric Network (132kV)", *American Journal of Engineering Research (AJER) e-ISSN: 2320-0847 p-ISSN : 2320-0936*, Vol. 4, Issue. 5, pp. 163-170.

[22] H. I. Hussein, G. A. Salman, and M. S. Hasan, "Phase measurement units based FACT's devices for the improvement of power systems networks controllability", *Int. J. Electr. Comput. Eng.*, Vol. 8, No. 2, pp. 888-899, 2018.

[23] M. Y. Suliman, "Voltage profile enhan- cement in distribution network using static synchronous compensator STATCOM", *Int. J. Electr. Comput. Eng.*, Vol. 10, No. 4, pp. 3367-3374, 2020.

[24] M. A. M. Faroug, D. N. Rao, R. Samikannu, S. K. Venkatachary, and K. Senthilnathan, "Comparative analysis of controllers for stability enhancement for wind energy system with STATCOM in the grid connected environment", *Renew. Energy*, Vol. 162, pp. 2408-2442, 2020.

[25] S. Sreedharan, T. Joseph, S. Joseph, C. V.

Received: January 4, 2022. Revised: March 24, 2022.

Chandran, Vishnu. J, and V. Das. P, "Power system loading margin enhancement by optimal STATCOM integration - A case study", *Comput. Electr. Eng.*, Vol. 81, p. 106521, 2020.

[26] L. Vanfretti and V. S. N. Arava, "Decision tree-based classification of multiple ope- rating conditions for power system Voltage stability assessment", *Int. J. Electr. Power Energy Syst.*, Vol. 123, No. April, p. 106251, 2020.

[27] B. B. Adetokun, C. M. Muriithi, and J. O. Ojo, "Voltage stability assessment and enhancement of power grid with increasing wind energy penetration", *Int. J. Electr. Power Energy Syst.*, Vol. 120, No. March, p. 105988, 2020.

[28] J. Qi, W. Zhao, and X. Bian, "Comparative Study of SVC and STATCOM Reactive Power Compensation for Prosumer Microgrids with DFIG-Based Wind Farm Integration", *IEEE Access*, Vol. 8, pp. 209878-209885, 2020.

[29] P. Wang, Y. Wang, N. Jiang, and W. Gu, "A comprehensive improved coordinated control strategy for a STATCOM integrated HVDC system with enhanced steady/transient state behaviors", *Int. J. Electr. Power Energy Syst.*, Vol. 121, No. August 2019, p. 106091, 2020.

[30] B. Ismail, N. I. A. Wahab, M. L. Othman, M. A. M. Radzi, K. N. Vijyakumar, and M. N. M. Naain, "A Comprehensive Review on Optimal Location and Sizing of Reactive Power Compensation Using Hybrid-Based Approaches for Power Loss Reduction, Voltage Stability Improvement, Voltage Profile Enhancement and Loadability Enhancement", *IEEE Access*, Vol. 8, pp. 222733-222765, 2020.

[31] G. Zhang, W. Hu, D. Cao, J. Yi, Q. Huang, Z. Liu, Z. Chen, and F. Blaabjerg "A data-driven approach for designing STATCOM additional damping controller for wind farms", *Int. J. Electr. Power Energy Syst.*, Vol. 117, No. September 2019, p. 105620, 2020.

[32] H. Bakir and A. A. Kulaksiz, "Modelling and Voltage control of the solar-wind hybrid micro-grid with optimized STATCOM using GA and BFA", *Eng. Sci. Technol. an Int. J.*, Vol. 23, No. 3, pp. 576-584, 2020.

[33] R. Jadeja, S. Patel, and S. Chauhan, "STATCOM - A Preface to Power Quality in Power Systems Performance", *Eng. Technol. Appl. Sci. Res.*, Vol. 6, No. 1, pp. 895-905, 2016.

[34] R. B. Magadum, N. R. Chitragar, S. N. Dodamani, and P. V. Gopikrishna, "Impact on Voltage Stability with Integration of Multiple STATCOM at Different Loading Conditions", In: *Proc. of ICDCS 2020 - 2020 5th Int. Conf. Devices, Circuits Syst.*, pp. 321-325, 2020.

[35] J. Sanam, "Optimization of planning cost of radial distribution networks at different loads with the optimal placement of distribution STATCOM using differential eVolution algorithm", *Soft Comput.*, Vol. 24, No. 17, pp. 13269-13284, 2020.

[36] L. Vanfretti and F. Milano, "Experience with PSAT (Power System Analysis Toolbox) as free and open-source software for power system education and research", *Int. J. Electr. Eng. Educ.*, Vol. 47, No. 1, pp. 47-62, 2010.

[37] M. G. Yenealem, L. M. H. Ngoo, D. Shiferaw, and P. Hinga, "Management of Voltage profile and power loss minimization in a grid-connected microgrid system using fuzzy-based STATCOM controller", *J. Electr. Comput. Eng.*, Vol. 2020, 2020.

Appendix

IEEE	Institute of Electrical and Electronics Engineers
p.u	Relative value system (Per unit)
CPF	Continuous power flow calculation
PSAT	Power System Analysis Toolbox
FACTS	Flexible Alternating Current Transmission System
STATCOM	Static Synchronous Compensator
V_{Sh}	Voltage (shunt) injected by the STATCOM
V_t	Line voltage
Qsh	Reactive power delivered by the STATCOM
Ish	Current (shunt) injected by the STATCOM
Λ	Load factor
TCSC	Thyristor controlled series compensator
SVC	Static var compensator
P_{G0}	Active power of generator
P_{L0}	Active load power
P_S	Supply bids
P_D	Demand bids
$(\delta_t \delta_{sh})$	Angle between the voltage
X	Line impedance.
g_{sh}	Equivalent conductance of STATCOM,
b_{sh}	Equivalent susceptibility of STATCOM
Z_{sh}	Equivalent impedance of STATCOM.
Q_{sh}	Reactive power of STATCOM.

 DOI: 10.22266/ijies2022.0630.37